Journal of Korean Society of
Coastal and Ocean Engineers
Vol. 12, No. 4, pp. 181~189, December 2000

Development of Weakly Nonlinear Wave Model and Its Numerical Simulation
약비선형 파랑 모형의 수립 및 수치모의

Jung Lyul Lee* and Chan Sung Park**
이정렬* · 박찬성**

Abstract ☐ A weakly nonlinear mild-slope equation has been derived directly from the continuity equation with the aid of the Galerkin's method. The equation is combined with the momentum equations defined at the mean water level. A single component model has also been obtained in terms of the surface displacement. The linearized form is completely identical with the time-dependent mild-slope equation proposed by Smith and Sprinks(1975). For the verification purposes of the present nonlinear model, the degenerate forms were compared with Airy(1845)'s non-dispersive nonlinear wave equation, classical Boussinesq equation, andsecond-order permanent Stokes waves. In this study, the present nonlinear wave equations are discretized by the approximate factorization techniques so that a tridiagonal matrix solver is used for each direction. Through the comparison with physical experiments, nonlinear wave model capacity was examined and the overall agreement was obtained.

Keywords **:** *Nonlinear Wave, Mild-Slope Equation, Exposed Breakwater, Submerged Breakwater*

要　旨 : 약비선형 완경사 방정식이 Galerkin 방법에 의하여 연속방정식으로부터 직접 유도되었으며 평균수면에서의 유속으로 표현된 운동방정식과 함께 사용된다. 두 방정식으로부터 수면변위 하나의 함수로 표현된 수식이 또한 유도되었으며 선형형은 Smith and Sprinks(1975)에 의하여 제안된 식과 일치하였고 천해, 천이영역, 심해 조건에 대하여 각각 *Airy(1845), Boussinesq, Stokes*의 2차 파랑과 비교되었다. 본 연구에서 유도된 비선형 파랑 방정식은 각 방향에 대하여 tridiagonal matrix를 얻기 위하여 근사적인 인수분해법으로 차분된다. 실험을 통하여 수립된 비선형 파랑 모형의 재현 능력을 검토하였으며 대체로 만족스러운 결과를 얻었다.

핵심용어 : 비선형파, 완경사 방정식, 차단식 방파제, 잠재방파제

1. INTRODUCTION

Early efforts to model wave transformation from offshore to onshore were based on the ray theory which accounts for wave refraction due to changes in bathymetry and the diffraction effects were ignored. Prediction of nearshore waves with the combined effects of refraction and diffraction as well as reflection has taken a new dimension with the use of the mild-slope equation and the Boussinesq equation. These two approaches in predicting nonlinear waves are essentially different in the sense that one is based on the linear wave characteristics and the other was started as an extensive work of the nonlinear shallow water waves.

1.1 Mild-Slope Equation Type

The mild-slope equation developed by Berkhoff (1972) has not only been used in its original form of an elliptic equation but also provided the basic governing equation for the development of other wave equations such as the parabolic equation (Radder, 1979), hyperbolic equation (Smith and Sprinks, 1975; Copeland, 1985; Madsen and Larsen, 1987), and elliptic equation of phase averaged type (Ebersole *et al.*, 1986).

*성균관대학교 토목환경공학과 (Dept. of Civil and Environmental Eng. , Sungkyunkwan University, Suwon Campus, Suwon 440-746, Korea)
**(주)도화종합기술공사 항만부(Dept. of Port and Coastal Eng., Dohwa Consulting Engineers Co., Ltd., Seoul 425-600, Korea)

Chamberlain and Porter (1995) proposed a modified mild slope equation that includes the higher-order bottom effect terms as well as the evanescent modes. As an effort towards modeling the propagation of nonlinear waves, recently several time-dependent mild slope equations have also been developed by Lee (1994), Nadaoka *et al.* (1994), and Isobe (1994).

Lee's Equation

Lee (1994) presented an equation set of nonlinear model for regular waves which can be applied to waves traveling from deep to shallow water.

$$\frac{\partial \eta}{\partial t}+\frac{1}{n}\nabla\cdot\left(\frac{nC^2}{g}\boldsymbol{u}\right)=0 \tag{1}$$

$$\frac{\partial \boldsymbol{u}}{\partial t}+\frac{1}{2}\nabla(\boldsymbol{u}\cdot\boldsymbol{u})+\frac{1}{2}\nabla\left(\frac{\partial \eta}{\partial t}\right)^2+g\nabla\eta=0 \tag{2}$$

whereis η the free surface displacement, $\boldsymbol{u}$ the horizontal velocity vector defined at the free surface level, n the ratio of the group velocity C_g to the phase speed C, and as the dispersion relationship $\sigma^2=gk\tanh kh$ is employed. The above equations completely satisfy the linear dispersion relationship and when expanded, they were proven to be consistent with Boussinesq equation of several types; Peregrine (1967), Madsen *et al.* (1991), and Nwogu (1993). In addition, the position of averaged velocity below the still water level was estimated based on the linear wave theory. For irregular waves, the following equation expressed in the alternative form of Smith and Sprinks (1975) instead of Eq. (1) is suggested.

$$\frac{\partial^2 \eta}{\partial t^2}+\nabla\cdot\left(\frac{CC_g}{g}\frac{\partial \boldsymbol{u}}{\partial t}\right)+(\sigma^2-k^2CC_g)\eta=0 \tag{3}$$

Nadaoka's Equation

Nadaoka *et al.* (1994) derived a time-dependent nonlinear dispersive wave equation with the multi-term coupling technique, which are here given in the single-term representation as

$$\frac{\partial \eta}{\partial t}+\nabla\cdot\left[\left(\frac{C^2}{g}+\eta\right)\boldsymbol{u}_o\right]=0 \tag{4}$$

$$CC_g\frac{\partial \boldsymbol{u}_o}{\partial t}+C^2\nabla\left[g\eta+\eta\frac{\partial w_o}{\partial t}+\frac{1}{2}(\boldsymbol{u}_o\cdot\boldsymbol{u}_o+w_o^2)\right]=$$
$$\frac{\partial}{\partial t}\left[\frac{C(C-C_g)}{k^2}\nabla(\nabla\cdot\boldsymbol{u}_o)+\nabla\left\{\frac{C(C-C_g)}{k^2}\right\}(\nabla\cdot\boldsymbol{u}_o)\right] \tag{5}$$

where $\boldsymbol{u}_o(u, v)$is the two-dimensional horizontal velocity vector and w_o the vertical velocity. The subscript 'o' denotes the value defined at $z=0$. The vertical velocity, w_o was given as

$$w_o=-\nabla\cdot\frac{\tanh kh}{k}\boldsymbol{u}_o \tag{6}$$

The C, C_g, and k are respectively the phase and the group velocity, and the wave numbers which are obtained by the linear dispersion relationship under the prescribed incident frequency σ and local depth h.

Isobe's Equation

Isobe (1994) also derived nonlinear mild-slope equation as given below by expanding the velocity potential into a series in terms of a given set of vertical distribution functions and hence include full nonlinearity and full dispersivity.

$$f_\alpha^\eta\frac{\partial \eta}{\partial t}+\nabla\cdot(A_{\alpha\beta}\nabla\hat{\phi}_\beta)-B_{\alpha\beta}\hat{\phi}_\beta+(C_{\beta\alpha}-C_{\alpha\beta})(\nabla\hat{\phi}_\beta)\cdot(\nabla h)$$
$$+\frac{\partial f_\beta^\eta}{\partial h}f_\alpha^\eta\hat{\phi}_\beta(\nabla\eta)\cdot(\nabla h)=0 \tag{7}$$

$$g\eta+f_\beta^\eta\frac{\partial\hat{\phi}_\beta}{\partial t}+\frac{1}{2}f_\gamma^\eta f_\beta^\eta(\nabla\hat{\phi}_\gamma)\cdot(\nabla\hat{\phi}_\beta)+$$
$$\frac{1}{2}\frac{\partial f_\gamma^\eta}{\partial z}\frac{\partial f_\beta^\eta}{\partial z}\hat{\phi}_\gamma\hat{\phi}_\beta+\frac{\partial f_\gamma^\eta}{\partial h}f_\beta^\eta\hat{\phi}_\gamma(\nabla\hat{\phi}_\beta)\cdot(\nabla h)=0 \tag{8}$$

where

$$f_\alpha^\eta=f_\alpha\Big|_{z=\eta},\quad\frac{\partial f_\alpha^\eta}{\partial z}=\frac{\partial f_\alpha}{\partial z}\Big|_{z=\eta}$$

$$A_{\alpha\beta}=\int_{-h}^{\eta}f_\alpha f_\beta dz,\ B_{\alpha\beta}=\int_{-h}^{\eta}\frac{\partial f_\alpha}{\partial z}\frac{\partial f_\beta}{\partial z}dz,C_{\alpha\beta}=\int_{-h}^{\eta}\frac{\partial f_\alpha}{\partial h}f_\beta dz$$

The unknowns are η and $\hat{\phi}_\alpha(\alpha=1$ to N). The vertical distribution of the velocity potential, ϕ, is expressed as a series in terms of a set of vertical distribution functions, f_α:

$$\phi(\boldsymbol{x},z,t)=\sum_{\alpha=1}^{N}\hat{\phi}_\alpha(\boldsymbol{x},t)f_\alpha(z;h(\boldsymbol{x}))\equiv\hat{\phi}_\alpha f_\alpha \tag{9}$$

where $\hat{\phi}_\alpha$ is the coefficient to f_α and therefore independent of z, and $\boldsymbol{x}=(x, y)$ denotes the position vector on the horizontal plane. The f_α is expressed in the terms of the local water depth $h(\boldsymbol{x})$ as is normally the case. It was also shown that nonlinear shallow water equations and Boussinesq equations as well as mild-slope equation can be derived as special cases of the nonlinear mild-slope equations.

As the simplest case, Eqs. (7) and (8) can be expressed by the single component as follows.

$$f^{\eta}\frac{\partial \eta}{\partial t}+\nabla(A\nabla\hat{\phi})-B\hat{\phi}=0 \tag{10}$$

$$g\eta+f^{\eta}\frac{\partial\hat{\phi}}{\partial t}+\frac{1}{2}(f^{\eta}\nabla\hat{\phi})^2+\frac{1}{2}\left(\frac{\partial f^{\eta}}{\partial z}\hat{\phi}\right)^2=0 \tag{11}$$

where $A=CC_g/g$, $B=(\sigma^2-k^2CC_g)/g$. If we assume $f(z)=\cosh k(h+z)/\cosh kh$ and $f^{\eta}\approx 1$, we obtain as

$$\frac{\partial \eta}{\partial t}+\nabla\left(\frac{CC_g}{g}\nabla\hat{\phi}\right)-\frac{\sigma^2-k^2CC_g}{g}\hat{\phi}=0 \tag{12}$$

$$\frac{\partial\hat{\phi}}{\partial t}+g\eta+\frac{1}{2}(\nabla\hat{\phi})^2+\frac{1}{2}w^2=0 \tag{13}$$

Therefore, the above can be consistent with Lee (1994)'s equation in single component expression.

1.2 Boussinesq Equation Type

The classical Boussinesq equations for one-dimensional propagation were first presented by Boussinesq(1872, 1877) and later the equations were extended to two-dimensional propagation over mildly sloping bottoms by Peregrine(1967). The Boussinesq type equations are known to simulate the combined effects of nonlinear short wave phenomena in shallow water areas quite well. Their major restriction, however, is to incorporate only weak dispersion and weak nonlinearity. Generally, the weak dispersion is more critical restriction as it directly affects the accuracy of both wave celerity and group velocity which is crucial for most wave dynamics. This problem has attracted considerable attention in the last 10 years. Numerous other formulations, therefore, have been developed to improve dispersion characteristics.

2. NONLINEAR VERSION OF MILD-SLOPE EQUATION

2.1 Derivation

The nonlinear mild-slope equation will be derived directly from the continuity equations by using the Galerkin's method. The continuity equations of an incompressible fluid are given by

$$\nabla\cdot\boldsymbol{u}+\frac{\partial w}{\partial z}=0 \tag{14}$$

where $\boldsymbol{u}$, w are the horizontal velocity and vertical velocity components, respectively. A bold face symbol indicates two horizontal components of flow vector; $\boldsymbol{u}=(u, v)$. The two-dimensional gradient operator $(\partial/\partial x, \partial/\partial y)$, is denoted by ∇. We multiply $f(z)$ to Eq. (14), and integrate from the bottom to the free surface.

$$\begin{aligned}&\int_{-h}^{\eta}f\nabla\cdot\boldsymbol{u}dz+\int_{-h}^{\eta}f\frac{\partial w}{\partial z}dz\\&=\int_{-h}^{\eta}\nabla\cdot(f\boldsymbol{u})dz-\int_{-h}^{\eta}\boldsymbol{u}\cdot\nabla f dz-\int_{-h}^{\eta}\left(\frac{\partial f}{\partial z}\right)^2dz\hat{\phi}\\&+\int_{-h}^{\eta}\frac{\partial}{\partial z}(fw)dz=0\end{aligned} \tag{15}$$

where, η is the free surface displacement and $\boldsymbol{u}$ is given by $\nabla\phi$ in terms of velocity potential. For the slowly varying water depth, the wave part of the velocity potential may be written as

$$\phi(\boldsymbol{x},z,t)=f(z)\hat{\phi}(\boldsymbol{x},t)$$

where $f(z)=\cosh k(h+z)/\cosh kh$ is a slowly varying function of $\boldsymbol{x}$ and $\hat{\phi}$ denotes the velocity potential at the mean water level, termed as 'the surface potential'. Recall Leibnitz's rule

$$\nabla\int_{\beta}^{\alpha}f dz=\int_{\beta}^{\alpha}\nabla f dz+f|_{\alpha}\nabla\alpha-f|_{\beta}\nabla\beta$$

to obtain the following expression from Eq. (15).

$$\begin{aligned}&\nabla\cdot\int_{-h}^{\eta}f^2dz\nabla\hat{\phi}-\int_{-h}^{\eta}\left(\frac{\partial f}{\partial z}\right)^2dz\hat{\phi}-[\nabla\eta\cdot f\boldsymbol{u}]_{\eta}\\&-[\nabla h\cdot f\boldsymbol{u}]_{-h}+[fw]_{\eta}-[fw]_{-h}=0\end{aligned} \tag{16}$$

Substituting the kinematic boundary conditions at free surface($z=\eta$) and at bottom($z=-h$) into Eq. (16),

$$w|_{\eta}-\frac{\partial\eta}{\partial t}-\boldsymbol{u}_{\eta}\cdot\nabla\eta=0 \tag{17}$$

$$w|_{-h}+\boldsymbol{u}_{-h}\cdot\nabla h=0 \tag{18}$$

we obtain

$$f_{\eta}\frac{\partial\eta}{\partial t}+\nabla\cdot\int_{-h}^{\eta}f^2dz\nabla\hat{\phi}-\int_{-h}^{\eta}\left(\frac{\partial f}{\partial z}\right)^2dz\hat{\phi}=0 \tag{19}$$

where f_{η} is the fvalue at the free surface. Taking Taylor series expansion about $\eta=0$ to Eq. (19),

$$\left(1+\eta\frac{\partial f}{\partial z}\right)_\eta\frac{\partial\eta}{\partial t}+\nabla\cdot\int_{-h}^{\eta}f^2dz\nabla\hat{\phi}-\int_{-h}^{0}\left(\frac{\partial f}{\partial z}\right)^2dz\hat{\phi}$$
$$+\nabla\cdot(\eta\nabla\hat{\phi})-\eta\left(\frac{\partial f}{\partial z}\right)_\eta\hat{\phi}=0 \tag{20}$$

where

$$\int_{-h}^{0}f^2dz=\frac{CC_g}{g}$$
$$\int_{-h}^{0}\left(\frac{\partial f}{\partial z}\right)^2dz=\frac{\sigma^2-k^2CC_g}{g}$$

and the second order term of the first term and the last term can be offset retaining the lowest-order nonlinear terms,

$$\left(\eta\frac{\partial f}{\partial z}\right)_\eta\frac{\partial\eta}{\partial t}\square\eta\left(\frac{\partial f}{\partial z}\right)_\eta\left(\frac{\partial f}{\partial z}\right)_\eta\hat{\phi}=\left(\frac{\partial f}{\partial z}\right)_\eta\left(\frac{\partial\phi}{\partial z}\right)_\eta \tag{21}$$

Therefore Eq. (22) can be the following equation:

$$\frac{\partial\eta}{\partial t}+\nabla\cdot\left[\left(\frac{CC_g}{g}+\eta\right)\boldsymbol{u}_o\right]-\frac{\sigma^2-k^2CC_g}{g}\hat{\phi}=0 \tag{22}$$

where $\boldsymbol{u}_o=\nabla\hat{\phi}$ as the horizontal velocity vector at $z=0$. Differentiating by the variable t:

$$\frac{\partial^2\eta}{\partial t^2}+\nabla\cdot\left[\left(\frac{CC_g}{g}+\eta\right)\left(\frac{\partial\boldsymbol{u}_o}{\partial t}\right)\right]+\nabla\cdot\left(\boldsymbol{u}_o\frac{\partial\eta}{\partial t}\right)$$
$$-\frac{\sigma^2-k^2CC_g}{g}\frac{\partial\hat{\phi}}{\partial t}=0 \tag{23}$$

where C, C_g, σ and k are assumed to be time independent. Substituting the dynamic free surface boundary condition,

$$\frac{\partial\hat{\phi}}{\partial t}+\frac{1}{2}(\boldsymbol{u}_o^2+w_o^2)+g\eta+\eta\frac{\partial w_o}{\partial t}=0 \tag{24}$$

and assuming the last terms in Eq. (24),

$$w_o\square\frac{\partial\eta}{\partial t} \tag{25}$$

respectively and then yield the following equation:

$$\frac{\partial^2\eta}{\partial t^2}+\nabla\cdot\left[\left(\frac{CC_g}{g}+\eta\right)\left(\frac{\partial\boldsymbol{u}_o}{\partial t}\right)\right]+\nabla\cdot\left(\boldsymbol{u}_o\frac{\partial\eta}{\partial t}\right)$$
$$+\frac{\sigma^2-k^2CC_g}{g}\left[\frac{1}{2}\boldsymbol{u}_o^2+g\eta+\eta\frac{\partial^2\eta}{\partial t^2}+\frac{1}{2}\left(\frac{\partial\eta}{\partial t}\right)^2\right]=0 \tag{26}$$

The above equation is combined with the nonlinear momentum equation defined at $z=0$.

$$\frac{\partial\boldsymbol{u}_o}{\partial t}+\nabla\left[g\eta+\int_0^\eta\frac{\partial w}{\partial t}dz+\frac{1}{2}(\boldsymbol{u}_\eta\cdot\boldsymbol{u}_\eta+w_\eta^2)\right]=0 \tag{27}$$

Taking Taylor series expansion about $\eta=0$ and retaining the lowest-order nonlinear terms, Eq. (27) becomes

$$\frac{\partial\boldsymbol{u}_o}{\partial t}+\nabla\left[g\eta+\eta\frac{\partial w}{\partial t}+\frac{1}{2}(\boldsymbol{u}_o\cdot\boldsymbol{u}_o+w_\eta^2)\right]=0 \tag{28}$$

at $z=0$ and then finally we obtain the following momentum equation:

$$\frac{\partial\boldsymbol{u}_o}{\partial t}+g\nabla\eta+\frac{1}{2}\nabla\boldsymbol{u}_o^2+\frac{3}{2}\nabla\left(\frac{\partial\eta}{\partial t}\right)^2=0 \tag{29}$$

Using the irrotationality,

$$\frac{\partial\boldsymbol{u}_o}{\partial t}+g\nabla\eta+\boldsymbol{u}_o\cdot\nabla\boldsymbol{u}_o+\frac{3}{2}\nabla\left(\frac{\partial\eta}{\partial t}\right)^2=0 \tag{30}$$

Therefore, Eqs. (26) and (30) are a set of the governing equations used for nonlinear wave propagation in this study. We used the Miche's criterion (Miche, 1951) because the breaking wave model is simple and accurate enough, and guarantees stability. For the mass conservation, the broken mass due to wave breaking is consequently passed on the next step elevation at each grid.

2.2 Single Component Model

Combining Eqs. (26) and (30), yields

$$\frac{\partial^2\eta}{\partial t^2}-\nabla\cdot\left[\frac{CC_g}{g}\nabla\left(g\eta+\frac{\boldsymbol{u}_o^2}{2}+\frac{3\sigma^2}{2}\eta^2\right)\right]+\nabla\cdot\left[\frac{\partial(\eta\boldsymbol{u}_o)}{\partial t}\right]$$
$$+\left[\frac{\sigma^2-k^2CC_g}{g}\right]\left[g\eta+\frac{\boldsymbol{u}_o^2}{2}+\frac{3\sigma^2}{2}\eta^2\right]=0 \tag{31}$$

In order to eliminate the velocity components except η, the following approximate relations are applied.

$$\boldsymbol{u}_o^2=\frac{g^2}{C^2}\eta^2,\ \frac{\partial(\eta\boldsymbol{u}_o)}{\partial t}=-g\nabla\eta^2$$

Then we obtain

$$\frac{\partial^2\eta}{\partial t^2}-\nabla\cdot\left[\frac{CC_g}{g}\nabla\left(g\eta+\frac{g^2\eta^2}{2C^2}+\frac{3\sigma^2}{2}\eta^2\right)\right]-g\nabla^2\eta^2$$
$$+\left[\frac{\sigma^2-k^2CC_g}{g}\right]\left[g\eta+\frac{g^2\eta^2}{2C^2}+\frac{3\sigma^2}{2}\eta^2\right]=0 \tag{32}$$

For the asymptotic analysis, the above is re-expressed as

$$\frac{\partial^2\eta}{\partial t^2} = \nabla\cdot\left[\frac{CC_g}{g}\nabla\left(g\eta+\frac{g^2\eta^2}{2C^2}\left(\frac{1}{2}+\frac{3}{2}\tanh^2 kh\right)\right)\right]+g\nabla^2\eta^2$$
$$-\left[\frac{k^2C^2(1-n)}{g}\right]\left[g\eta+\frac{g^2\eta^2}{C^2}\left(\frac{1}{2}+\frac{3}{2}\tanh^2 kh\right)\right] \quad (33)$$

We shall now consider the special forms of Eq. (33) when depth is relatively shallow and deep. In the very shallow water so that $C = C_g = \sqrt{gh}$ and tnah²kh□0, Eq. (33) becomes

$$\frac{\partial^2\eta}{\partial t^2} = g\nabla\cdot(h\nabla\eta)+\frac{g}{2}\nabla\cdot\left(h\nabla\frac{\eta^2}{h}\right)+g\nabla^2\eta^2 \quad (34)$$

which may be shown to be the combined form of Airy(1845)'s non-dispersive nonlinear wave equations for varying depth, correct to the second-order in nonlinearity.

Next, the phase speed and the group velocity are given in lowest-order dispersion as

$$C = \sqrt{gh}(1-k^2h^2/6) \text{ and } C_g = \sqrt{gh}(1-k^2h^2/2)$$

Replacing them should result in the combined version of Boussinesq equation.

$$\frac{\partial^2\eta}{\partial t^2} = \nabla\cdot\left[\frac{gh\left(1-\frac{k^2h^2}{6}\right)\left(1-\frac{k^2h^2}{2}\right)}{g}\nabla\left(g\eta+\frac{g^2\eta^2}{2gh\left(1-\frac{k^2h^2}{6}\right)^2}\right)\right]$$
$$+g\nabla^2\eta^2-\left[\frac{k^2gh\left(1-\frac{k^2h^2}{6}\right)^2-k^2gh\left(1-\frac{k^2h^2}{2}\right)\left(1-\frac{k^2h^2}{6}\right)}{g}\right]$$
$$\left[g\eta+\frac{g^2\eta^2}{2gh\left(1-\frac{k^2h^2}{6}\right)^2}\right]$$
$$\equiv\nabla\cdot\left[h\left(1-\frac{2}{3}k^2h^2\right)\nabla\left(g\eta+\frac{g\eta^2}{2h(1-k^2h^2/3)}\right)\right]+g\nabla^2\eta^2$$
$$-k^2h\left(\frac{k^2h^2}{3}\right)\left[\frac{g\eta^2}{2h(1-k^2h^2/3)}\right] \quad (35)$$

Retaining the leading order,

$$\frac{\partial^2\eta}{\partial t^2} = g\nabla\cdot(h\nabla\eta)\cdot\frac{2g}{3}\nabla\cdot(k^2h^3\nabla\eta)$$
$$+\frac{g}{2}\nabla\cdot\left(h\nabla\frac{\eta^2}{h}\right)+g\nabla^2\eta^2-\frac{k^4h^3}{3}g\eta \quad (36)$$

For the constant depth, invoking the relation $k^2h = \nabla^2\eta$,

$$\frac{\partial^2\eta}{\partial t^2} = g\nabla\cdot(h\nabla\eta)-\frac{1}{3}(gh)^3k^2-\frac{3g}{3}\nabla^2\eta^2 \quad (37)$$

which is in accordance with the classical Boussinesq approximations.

For the deep water of constant depth, $C = \sqrt{g/k}$ and $C_g = C/2$. In this case, Eq. (33) can be approximated as

$$\frac{\partial^2\eta}{\partial t^2} = \frac{g}{k}\nabla^2\eta+\frac{5}{2}g\nabla^2\eta^2 \quad (38)$$

with $k^2\eta^2$□-$\nabla^2\eta^2/4$ based on the Stokes wave theory.

If Eq. (31) is linearized, the time-dependent mild-slope equation proposed by Smith and Sprinks (1975) is obtained as

$$\frac{\partial^2\eta}{\partial t^2}-\nabla\cdot[CC_g\nabla\eta]+[\sigma^2-k^2CC_g]\eta = 0 \quad (39)$$

2.3 Numerical Analysis

The governing equations (26) and (30) have the similar form to a set of the following shallow water equations.

$$\frac{\partial\eta}{\partial t}+\nabla\cdot[(h+\eta)\boldsymbol{u}_o] = 0 \quad (40)$$

$$\frac{\partial\boldsymbol{u}_o}{\partial t}+g\nabla\eta+\boldsymbol{u}_o\cdot\nabla\boldsymbol{u}_o = 0 \quad (41)$$

There are already a number of numerical schemes to provide the accurate and stable results in solving the above shallow water equations, differently from Nadaoka et al. (1994)'s equations which appeared to have difficulty in obtaining numerical solutions. If Eq. (40) is differentiated by time t, we obtain

$$\frac{\partial^2\eta}{\partial t^2}+\nabla\cdot\left[(h+\eta)\frac{\partial\boldsymbol{u}_o}{\partial t}\right]+\nabla\cdot\left[\boldsymbol{u}_o\frac{\partial\eta}{\partial t}\right] = 0 \quad (42)$$

In very shallow water, therefore, Eqs. (26) and (30) are identical with Eqs. (42) and (41), respectively.

They are discretized by the approximate factorization techniques so that a tridiagonal matrix solver is used for each direction. In this paper, the detailed description on numerical scheme is omitted since a number of similar schemes have been represented so far. Since the time step of an explicit scheme is very strictly limited by the Courant-Friedrichs-Lawy (CFL) condition, it is advisable to use the implicit scheme without such concern. The momentum equations, which have the nonlinear advective

term, are divided into the two elementary operations; advection and propagation, and solved by using a fractional step method. The fraction step method is based on the recognition that the physical phenomena of water flow can be represented by superimposing individual operations as Chorin (1968) pointed out.

3. PHYSICAL EXPERIMENTS

The experiment was conducted in a Coastal-Hydraulics Laboratory wave flume of Sungkyunkwan University, in order to verify the numerical results of nonlinear waves. The wave flume of 50 cm deep, 40 cm wide, and 12 m long consists of a wave generator and beach zones. The bottom and side walls of the flume are glass to allow easy optical access. The regular waves were generated by a piston-type wave paddle and the beach slope of 1/19 was set at the other end of the wave flume.

The wave flume was decorated with the data acquisition system accessing the wave profile signals from the wave gages. Gages were connected with amplifier for increasing analog signals. Then the DaqBoard 100A (DaqBoard), A/D converter, changes conditioned signals into corresponding digital numbers saved as ASCII format.

Physical experiments were accomplished for two cases. Experimental conditions consist of same wave conditions for two different experimental setup, respectively. Wave conditions for Case 1-A and Case 2-A are T=0.8sec, Hi= 2 cm, Ur=10.05 and steepness=0.0282. Wave conditions for Case 1-B and Case 2-B are T=1.0 sec, Hi=1.5cm, Ur=12.80 and steepness= 0.0162. The Ursell parameter is a dimensionless parameter that is useful to define the range of application of the various wave theories. Generally cnoidal theory is applicable for Ur > 25 and Stokes theory is applicable for Ur < 10.

The layouts of two different experimental configurations are illustrated in Figs. 1 and 2 with the locations of the measurement stations and detailed geometry of the flume. The exposed breakwater is placed to the left half of the wave tank looking in the direction of the wave propagation, while the submerged breakwater is placed to the left side.

As shown in Fig. 1, wave gages 1, 2 and 3 for Case 1 were located at x = 41 cm, x = 81 cm and x = 121cm mea-

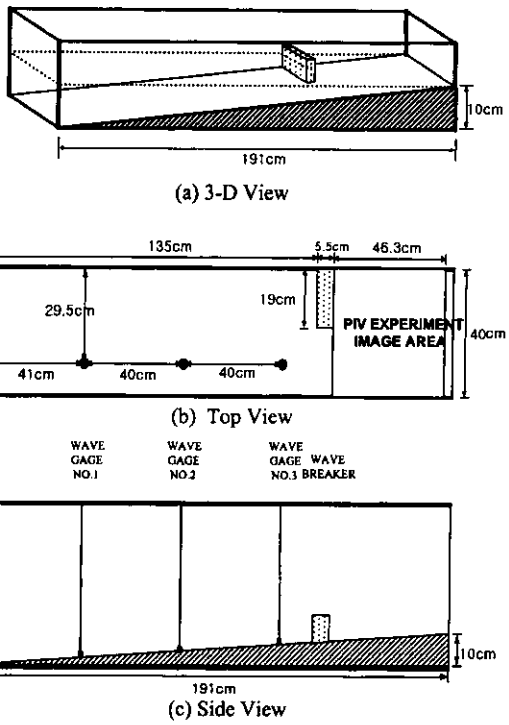

Fig. 1. Physical layout of experiment Case 1: (a) 3-D view, (b) top view, (c) side view.

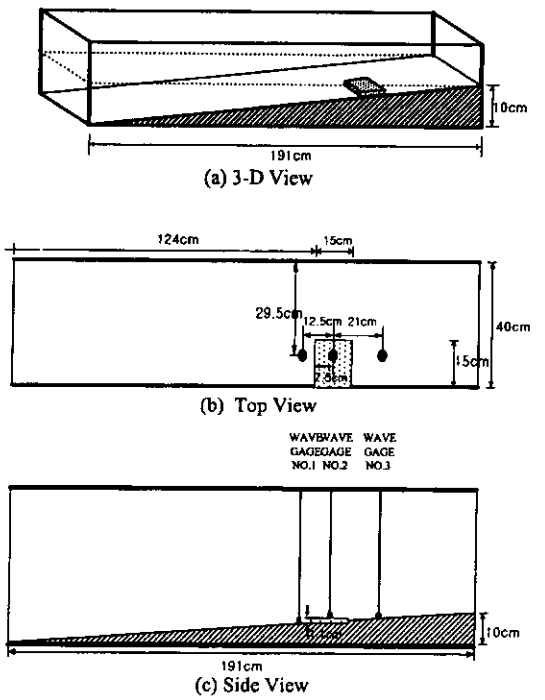

Fig. 2. Physical layout of experiment Case 2: (a) 3-D view, (b) top view, (c) side view.

sured shoreward from the toe of slope, respectively. The measuring section was located about 10.5 cm apart from the nearer sidewall.

As for the submerged breakwater shown in Fig. 2. wave gages 1, 2 and 3 were located at x = -21.5 cm, x = 0 cm (center) and x = 12.5 cm measured shoreward from the center of submerged breakwater, respectively. The squared submerged breakwater is impermeable and has 1.1 cm height and 15 cm length.

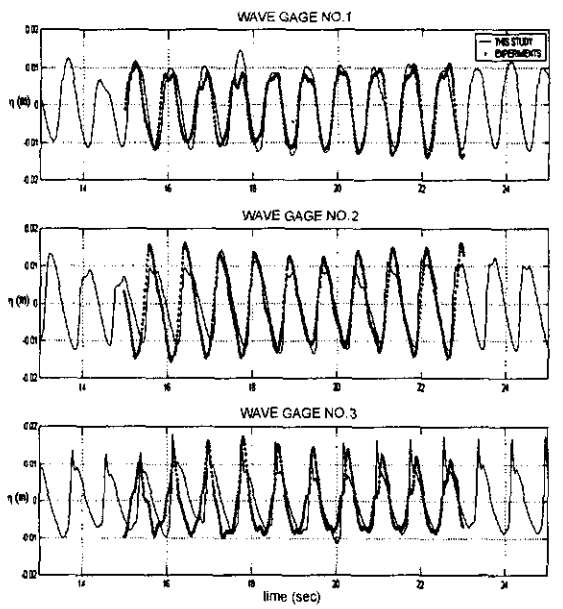

Fig. 3. Comparison of wave profiles at wave gages No. 1, 2 and 3 of Case 1-A (Hi=2.0 cm, T=0.8 s).

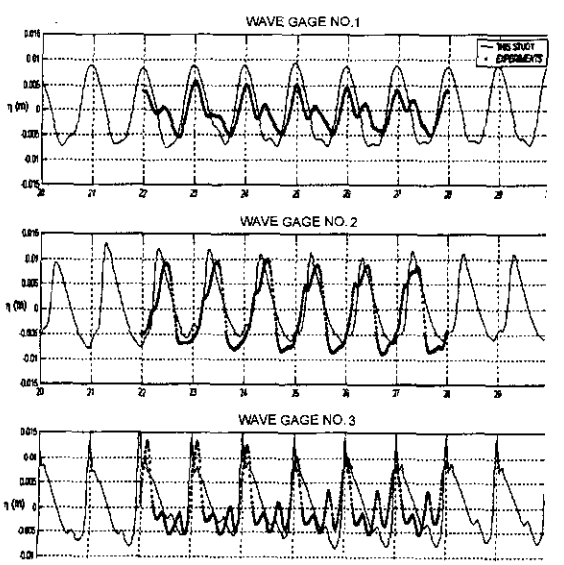

Fig. 4. Comparison of wave profiles at wave gages No. 1, 2 and 3 of Case 1-B (Hi =1.5 cm, T=1.0 s).

4. RESULTS

Figures 3 and 4 show a comparison between the observed and calculated temporal wave profiles for Case 1. The time series were synchronized with the computations at station 1. The measured results are also shown in each figure by closed circles. The agreement appears to be generally acceptable, though it is evident that both results show the weak irregularity. In Case 1-A, the waves measured at stations 2 and 3 show the strong asymmetry due to nonlinearity as we expected. While several peaks in a period are shown in Case 1-B experiments, differently from the numerical prediction. Judging from the detailed experiments using a moving cart, they seemed to be caused by reflection of asymmetric waves (radiating from a breakwater) rather than the wave decomposition. Such multi-peaks can occur under wave decomposition. The wave decomposition is usually caused by a nonlinear wave train passing over a submerged bar or a submerged shelf. In this case, however, there is no submerged shelf but a breakwater causes the strong reflection. Figures 5 and 6 show the 3-D perspective views of instantaneous water surface elevation for two different wave conditions obtained from the numerical model. In those figures, the

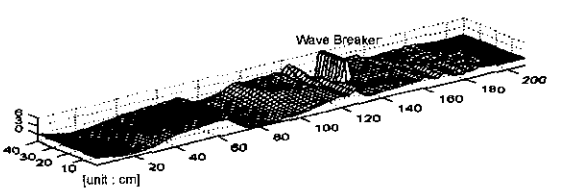

Fig. 5. 3-D view of nonlinear wave propagation by numerical model for Case 1-A.

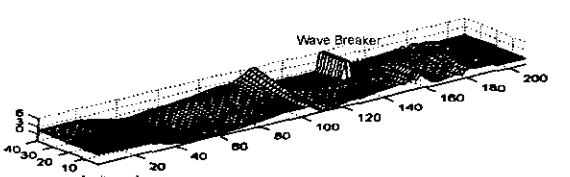

Fig. 6. 3-D view of nonlinear wave propagation by numerical model for Case 1-B.

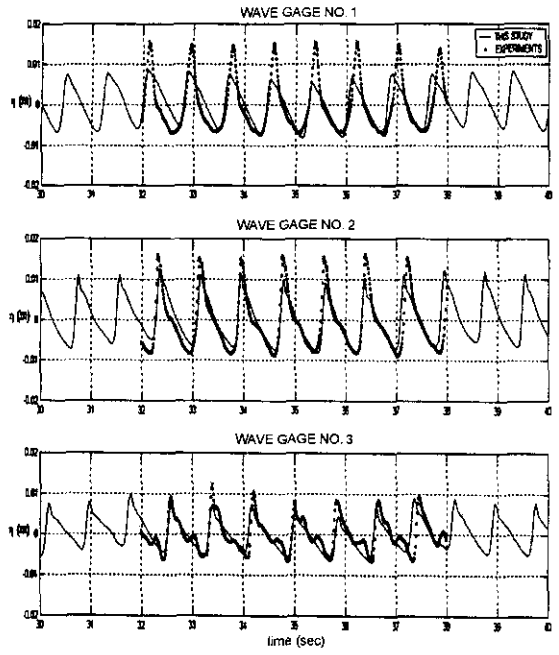

Fig. 7. Comparison of wave profiles at wave gages No. 1, 2 and 3 of Case 2-A (Hi =2.0 cm, T=0.8 s).

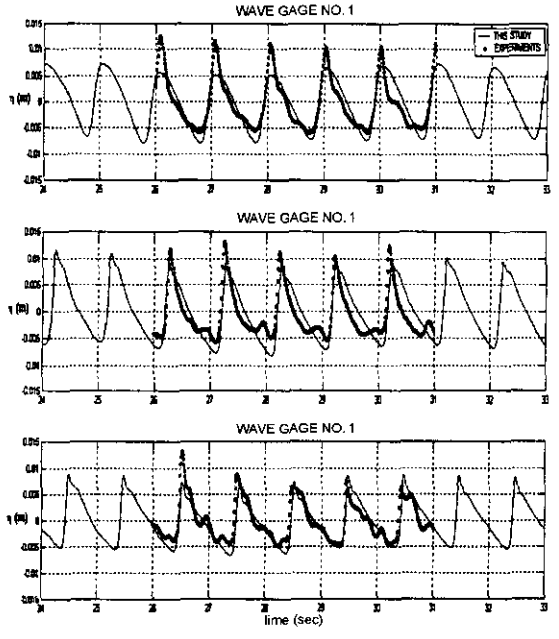

Fig. 8. Comparison of wave profiles at wave gages No. 1, 2 and 3 of Case 2-B (Hi =1.5 cm, T=1.0 s).

wave diffraction is shown behind a breakwater.

Figures 7 and 8 give the comparison of temporal wave profiles for Case 2. The numerical results are in good agreement with those of the observed data. Figures 9 and 10 show the 3-D views of instantaneous water surface elevation for two different wave conditions obtained from the numerical model. It is shown in Figs. 9 and 10 that wave profiles are deformed over the submerged breakwater section. The submerged breakwater seems to cause neither the strong wave decomposition nor predominant multi-peaks because its height is relatively thin.

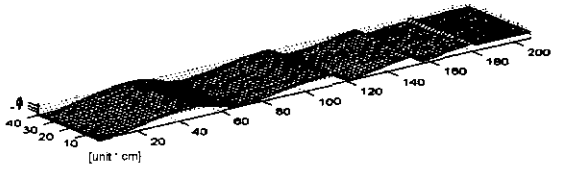

Fig. 9. 3-D view of nonlinear wave propagation by numerical model for Case 2-A.

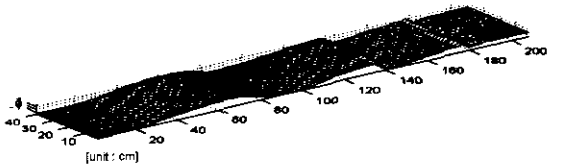

Fig. 10. 3-D view of nonlinear wave propagation by numerical model for Case 2-B.

5. CONCLUSION

The nonlinear mild-slope equation was derived directly from the continuity equation by using the Galerkin's method. In modeling breaking waves we employed the Miche's criterion which believed to be simple, stable, and reliable.

We verified nonlinear wave model capacity through comparison of numerical simulation to physical experiments for two configurations; the exposed breakwater and the submerged breakwater. The overall agreement appeared for the exposed breakwater, though it is evident that the weak irregularity in experimental data measurements showed. The waves showed strong asymmetry due to nonlinearity and multi-peaks due to reflection of nonlinear waves. Such phenomena might increase with Ursell parameter increasing.

In the submerged breakwater, the best agreement was shown. Wave profiles appeared to be deformed due to a

submerged breakwater. However, neither wave decomposition nor multi-peaks seems to be strongly observed in the case of the submerged breakwater because its height is relatively thin.

ACKNOWLEDGMENTS

Funding for this research from Korea Science and Engineering Foundation(KOSEF 961-1204-017-1) is gratefully acknowledged.

REFERENCES

Airy, G.B., 1845. Tides and waves, Encyclopedia Metropolitana, Art. 192, London.

Berkhoff, J.C.W., 1972. Computation of combined refraction-diffraction, *Proc. 13rd Int. Conf. Coastal Engrg.*, ASCE, pp. 471-490.

Boussinesq, J., 1872. Theorie des ondes et des remous qui se propagent le long d'un canal rectangulaire horizontalen communiquant au liquide continue dans cd canal des vitesse sensibliement pareilles de la surface du fond, *J. Math. Pure et Appliqué*, 2nd Series, **17**, pp. 55-108.

Boussinesq, J., 1877. Essai sur la theorie des eaux courantes, Memoires presentes par Divers Savants a L'Acad, *Sci. Inst. France, Series* 2. **23**(1), pp. 680.

Chamberlain, P.G. and Porter, D., *1995*. The modified mild-slope equation, *J. Fluid Mech.*, **291**, pp. 393-407.

Chorin, A.J., 1968. Numerical solution of the Navier-Stokes equations, *Math. Comput.*, **22**, pp. 745-762.

Copeland, G.J.M., 1985. A practical alternative to the mild slope wave equation, *Coastal Engrg.*, **9**, pp. *125-149.*

Ebersole, B.A., Cialone, M.A. and Prater, M.D., 1986. Regional coastal processes numerical modeling system, Report 1, RCPWWAVE-A linear wave propagation model for engineering use, Technical report CERC-86-4, US Army Engineer WES, Vicksburg, Mississippi.

Isobe, M., 1994. Time-dependent mild-slope equations for random waves, *proc. 24th Int. Conf. Coastal Engrg.*, ASCE, pp. 285-299.

Lee, J.L., 1994. Derivation of nonlinear model for irregular waves on mild slope, *J. Korea. Soc. Coast. and Ocean Eng.*, KSCOE, **6**(3), pp. 281-289.

Madsen, P.A. and Larsen, J., 1987. An efficient finite-difference approach to the mild-slope equation, *Coastal Engrg.*, **11**, pp. 329-351.

Madsen, P.A., Murray, R. and Sorensen, O.R., 1991. A new form of the Boussinesq equations with improved linear dispersion characteristics, *Coastal Engrg.*, **15**, pp. 371-388.

Miche, R., 1951. The reflecting power of maritime works exposed to action of the waves, Annals of the Highway Dept., National Press, France.

Nadaoka, K., Beji, S. and Nakagawa, Y., 1994. A fully-dispersive weaklynonlinear wave model and its numerical solutions, *Proc. 24th Int. Conf. on Coastal Engrg.*, ASCE, pp. 427-441.

Nwogu, O., 1993. An alternative form of the Boussinesq equations for nearshore wave propagation, *J. Waterway, Port, Coastal and Ocean Engrg.*, **119**, pp. 618-638.

Peregrine, D.H., 1967. Long waves on a beach, *J. Fluid Mech.*, **27**(4), pp. 815-827.

Radder, A.C., 1979. On the parabolic equation method for water-wave propagation, *J. Fluid Mech.*, **95**, pp. 159-176.

Smith, R. and Sprinks, T., 1975. Scattering of surface waves by a conical island, *J. Fluid Mech.*, **72**, pp. 373-384.